

ACTIVE DAMPER SYSTEM DESIGN AND CONTROL – PART B

Rafael Luís Teixeira*
rafael@mecanica.ufu.br

Francisco Paulo Lépoire Neto*
fplepoire@mecanica.ufu.br

José Francisco Ribeiro*
jrribeiro@mecanica.ufu.br

*Federal University of Uberlândia – College of Mechanical Engineering - Campus Santa Mônica 38400-089, Uberlândia-MG

Abstract. This paper presents the design of a control system applied to an active damper installed at a vehicle suspension. A two-degree of freedom discrete mechanical system is used to represent $\frac{1}{4}$ of the vehicle. A flexible metallic bellows that pumps fluid through a controlled valve and produces a reactive damping force constitutes the active damper. A piezoelectric actuator controls the size of the valve orifice. The hydrodynamic model of this damper, and the resulted nonlinear forces acting at the bellows and at the valve core are presented by the part A of this paper. The space state model of the vehicle dynamics and the LQG technique are used to design the global controller that estimates the valve orifice size associated with the optimum damping force required by the vehicle desired performance. The resulted orifice optimum size is used as the reference of a PID controller, which is designed to control the position of the piezoelectric actuator. The efficiency of the controllers is analyzed by numerical simulations of the vehicle under excitations generated by the rolling track.

Keywords: active damper; optimum control; PID

1. Introduction

Digital microcomputers and micro controllers are widely used to control engineering systems. The development of new actuators and inexpensive sensors provide the improvement on the design of robust and adaptive controllers, capable to deal with temporal parametric modifications of the system. This is the case of automotive active suspensions, where vibration control is implemented to achieve the ride confort, and or, to improve the vehicle dynamic stability. Several strategies were investigated: Kipling et al. (1998), Hagopian et al. (1999), Gilioomee & Els (1998) applied optimum control and state estimators of the vehicle dynamics associated with classic PID controllers to set the optimum damping force to be applied at the suspension. Using the same approach Ho & Sho (1999) and Yoshimura (1998) used a fuzzy controller to adjust a multiple stage valve of a damping device. In this case, each stage corresponds to a discrete damping coefficient imposed to the vehicle suspension.

The main proposal of this work is to control vehicle vibrations induced by rolling track irregularities. A two-degree of freedom discrete mechanical system is used to represent $\frac{1}{4}$ of the vehicle. The active damper model has one degree of freedom and is installed at the vehicle suspension. The proposed active damper uses a metallic flexible bellows, replacing the hydraulic piston of a conventional active suspension vehicle. The bellows geometrical configuration can be designed to provide the required axial displacement and stiffness ranges, under nominal internal pressure, to improve produced fluid flow. The damping force is generated when the fluid flows through an orifice whose size can be adjusted by a servo-valve. A piezoelectric linear actuator is used to control the orifice size. This device presents better dynamic response than that of the inductive electrodynamic actuators. The damping force and the reaction force applied at the valve core are nonlinear functions of the valve orifice size (GAP) and of the input velocity of the bellows (V_x), which is the relative velocity of the vehicle suspension. The fluid dynamic behavior of device modeled by finite element method, is present in the part A of this paper (Teixeira et. al, 2003) and is used to calculated the resulting forces at the bellows and at the valve core. Direct neural fuzzy models estimate these forces for combinations of GAP and V_x , and inverse analytical models estimates the GAP using combinations of the forces and of the input velocity V_x .

A PID control is designed to set the position of the valve core, defining the orifice size required to generate the optimum damping force at the vehicle suspension. This optimum force is obtained by the LQR theory, applied to the $\frac{1}{4}$ vehicle dynamic model. This way, the control system has hierarchical approach, since the vehicle and the damping device constitute two dynamic systems, coupled by the nonlinear hydrodynamic forces.

Numerical simulations are carried out to analyze the dynamic behavior of the vehicle submitted to excitations applied by the road profile. The passive model uses the maximum value that can be set by the damping device, corresponding to the smaller valve orifice. In this case the dynamic model of the valve is not taken into account. A second group of simulations use the active control system designed for two different values of the performance index admitted for the vehicle response. This index set the minimum value of the velocity V_x for which the control is active.

Next session presents the dynamic models of the vehicle and of the piezoelectric valve, and the hierarchical control strategies applied to the system. Numerical simulations results are shown in session 3, and some conclusions are presented in session 4.

2. Dynamic models and control strategies

The passive system is represented by Figure 1, where system dynamic matrix A is time invariant, since the damping coefficient provided by the damping device has constant value. This value corresponds to the minimum orifice size resulting maximum damping coefficient. In all simulations of the passive model the piezoelectric actuator is fixed and the valve dynamics is not considered. The neural fuzzy model, presented in Part A, is used to estimate the damping force at the bellows, for a constant GAP value and any V_x value. The irregularities of the rolling track (W) excite the tyre of the vehicle.

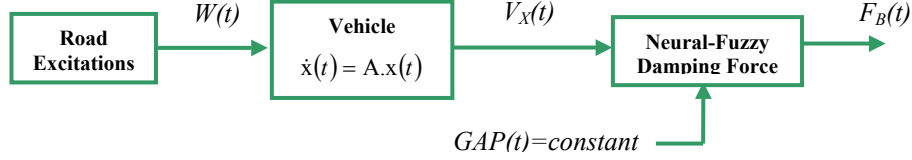


Figure 1: Passive system.

The state space single-input-multi-output system model is used to represent the vehicle, whose physical parameters are adopted to design the optimum control. All variables are measurable and the optimum control law is obtained by linear combination of the state, so that the standard quadratic cost functional is minimized (Franklin et. al, 1997; Athans, 1971).

The valve core is coupled to the piezoelectric actuator and the resultant system is modeled by one degree of freedom dynamic system. The valve PID controller design is based on the relay feedback test. (Cardoso and Ribeiro, 2003).

The proposed hierarchical control strategies are illustrated on Figure 02 and described by the following steps:

STEP 1. This step is realized off-line. Initially, the damping coefficient of the vehicle suspension has the lowest value. Using this value and the mass and stiffness parameters the dynamic matrix is defined and used to obtain the optimum control law. The valve core positioning PID self-tuning controller is designed.

STEP 2. From the initial condition and track excitations the vehicle state (x) is estimated and the relative velocity (V_x) at the bellows is obtained.

STEP 3. The LQR model using the state (x) calculates the optimum damping force (u). The damping coefficient variation (ΔC) is calculated by $u(t)/V_x(t)$. The absolute value of the damping rate ($\Delta C/\Delta t$) is limited to 30,400 (N.s/m)/s. Then the new damping coefficient ($C_{optimum}$) necessary to generate the optimum force is the actual damping (C_{actual}) plus the variation (ΔC). From this new damping coefficient the analytical inverse model estimates the reference GAP.

STEP 4. The designed PID controller will act on the piezoelectric valve to set the reference GAP. The valve dynamics response is calculated using the PID control action and the hydrodynamic force estimated by the valve neural-fuzzy model. This calculation is performed using the last available GAP and the actual relative velocity

STEP 5. The direct neural-fuzzy damping force model, using the resulted GAP value and the actual relative velocity obtains the actual damping force. Physically, this real force divided by the actual relative velocity is the actual damping coefficient to be imposed to the system. Then, the vehicle dynamic model is updated and is represented by $\dot{x}(t) = \hat{A}.x(t)$. This new dynamic matrix is used in the next simulation and the control process returns to STEP 2 with system actual state.

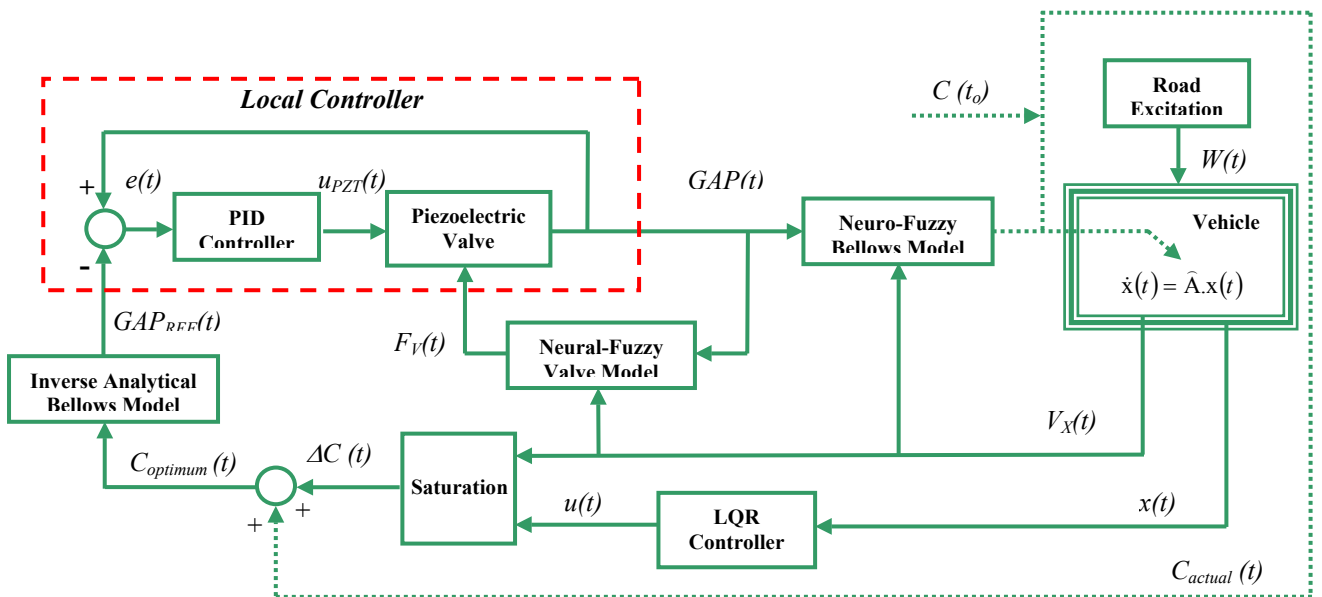


Figure 2: Active System.

To design the optimum control law, the mathematical model of the ¼ vehicle is described by the following linear differential equation; where x is the state vector, u is the control command, $A_{n \times n}$ e $B_{n \times m}$ are the dynamic matrices of the system, with n state variables and m actuators.

$$\dot{x}(t) = A.x(t) + B.u(t)$$

The optimization problem is formulated as follow: determine $u(t)$, with $t \in [0; \infty]$, which minimize the following quadratic cost functional J , where $Q_{n \times n}$ is a diagonal positive semi-definite matrix which weights the state x and $R_{n \times m}$ is positive definite that weights u .

$$J = \int_0^{\infty} [x(t)^T Q x(t) + u(t)^T R u(t)] dt$$

The optimal control vector (u) is the related to the state vector by means of the linear time varying feedback relationship:

$$u(t) = -K.x(t)$$

where $K_{n \times m}$ is a time varying control gain matrix given by:

$$K = R^{-1}.B.G$$

where $G_{n \times n}$ is the solution of the Riccati matrix algebraic equation:

$$K.B.R^{-1}.B'.G - G.A - A'.K - Q = 0$$

The existence and uniqueness of solution of this problem are guaranteed if $[A,B]$ is a controllable pair. Under this assumption the closed-loop system is asymptotically stable in the large, i.e., all of the eigen-values of $[A-B.K]$ are in the left-half complex plane. The structure of the time-invariant deterministic control system is shown in figure 3.

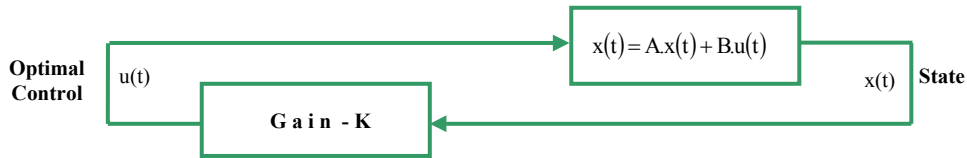


Figure 3. Deterministic feedback control system structure.

The two degrees of freedom ¼ vehicle dynamic model is represented by its state x . To develop the mathematical model, with the proposed damping device C_B installed at the suspension, consider the physical system illustrated on Figure 4, where M_S is the car body mass, M_R is the mass of the wheel, C_P and K_P are the tyre damping and stiffness coefficients and K_S is the suspension stiffness.

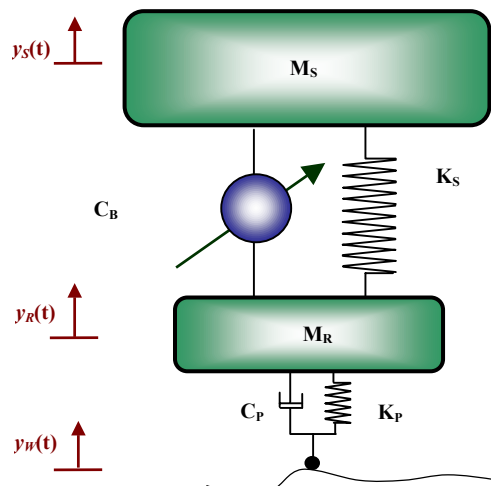


Figure 4: ¼ Equivalent vehicle model.

Applying the second Newton's Law, to the physical model, assuming: $y_s(t) > y_R(t) > y_w(t)$ and $\dot{y}_s(t) > \dot{y}_R(t) > \dot{y}_w(t)$, results:

$$M_S \ddot{y}_S + K_S (y_S - y_R) + c_B (\dot{y}_S - \dot{y}_V) + u = 0 \quad (1)$$

$$M_R \ddot{y}_R - K_S (y_S - y_R) - c_B (\dot{y}_S - \dot{y}_V) + K_P (y_R - y_W) + C_P (\dot{y}_R - \dot{y}_W) - u = 0$$

Defining the state vector by Equation (2) and using Equations (1), the mathematical model of the system state space is represented by Equation (3).

$$x = [y_S \quad y_R \quad \dot{y}_S \quad \dot{y}_R]^T \quad (2)$$

$$\begin{Bmatrix} \dot{y}_S \\ \dot{y}_R \\ \ddot{y}_S \\ \ddot{y}_R \end{Bmatrix} = \begin{bmatrix} 0 & 0 & 1 & 0 \\ 0 & 0 & 0 & 1 \\ -K_S/M_S & K_S/M_S & -C_B/M_S & -C_B/M_S \\ K_S/M_R & -(K_S + K_P)/M_R & C_B/M_S & -(C_B + C_P)/M \end{bmatrix} \begin{Bmatrix} y_S \\ y_R \\ \dot{y}_S \\ \dot{y}_R \end{Bmatrix} + \begin{bmatrix} 0 \\ 0 \\ 1/M_S \\ -1/M_R \end{bmatrix} \cdot \{u\} + \begin{bmatrix} 0 \\ 0 \\ 0 \\ 1/M_R \end{bmatrix} \{w\} \quad (3)$$

where:

$$w = K_P y_W + C_P \dot{y}_W \quad \text{and} \quad u = \Delta C_B (\dot{y}_S - \dot{y}_R)$$

Equation 3 is rewritten in the compact form of Equation (4) and the solution is obtained applying some initial condition $x(t=0)$.

$$\dot{x}(t) = \begin{bmatrix} 0 & I \\ KM^{-1} & CM^{-1} \end{bmatrix} x(t) + \begin{bmatrix} 0 \\ M^{-1} \end{bmatrix} u(t) + G \cdot w(t) \quad (4)$$

The piezoelectric actuator and the valve core constitute a one-degree of freedom system with natural frequency ω_n much larger than the vehicle natural frequencies. Equation (5) shows the system transfer function that relates the valve core displacement (GAP) with the control force U_{PZT} applied by the piezoelectric actuator. The control voltage at the PZT electrodes produces this force. The damping factor and the stiffness are ξ_v and K_v , respectively.

$$G_{\text{valve}}(s) = \frac{GAP(s)}{U_{PZT}(s)} = \frac{1}{K_V} \left[\frac{\omega_n^2}{s^2 + 2\xi_v \omega_n s + \omega_n^2} \right] \quad (5)$$

Figure 5 shows the block diagram of the piezoelectric valve PID control system. The error $e(t)$ is determined by the difference between the reference GAP_{REF} , defined by the LQR control, and the actual valve position GAP. The hydrodynamic force applied at the valve core is the nonlinear excitation, represented by F_{VALVE} .

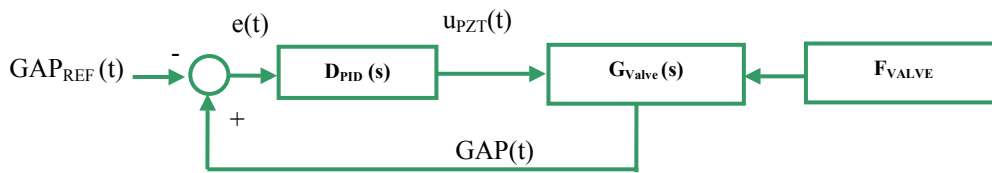


Figure 5: Local PID control diagram

The PID control law formulation in the time domain is represented by equation 6:

$$u(t) = KP e(t) + KI \int_0^t e(\tau) d\tau + KD \frac{de(t)}{dt} \quad (6)$$

The controller parameters KP , KD and KI are determined by simplified method of the relay feedback test (Cardoso and Ribeiro, 2003). In this method are identified the DC gain of the system and the gain close to the natural frequency. PID controller's gains are found minimizing the error between the response of the system+controller and one desired open loop frequency response specified by design conditions, as for example: frequency band of the control action, closed loop damping factor, settling time.

3. Numerical Simulations

Numerical simulations are carried out to analyze the dynamic behavior of the vehicle submitted to excitations applied by the road irregularities. Table 1 shows the physical parameters adopted for all simulations. The active system response is calculated using two different values of the vehicle performance index and is compared to the passive system response. The difference of each active system is the limitation imposed to the maximum relative velocity of suspension (V_x), i.e., if the absolute value of the relative velocity is larger than given performance index, the suspension is activated, otherwise the control system sets the valve totally open, imposing to the system the smallest damping. In the passive system simulation the C_B damping coefficient is fixed at its maximum value. In all active simulations the initial value of C_B is set to 450 Ns/m, which corresponds to the maximum valve orifice size.

Table 1: System Physical Parameters.

M_S	Quarter Vehicle Body Mass	300 Kg
M_R	Wheel Mass	25 Kg
M_V	Piezoelectric Valve Mass	0.200 Kg
K_S	Passive Suspension Stiffness	18000 N/m
K_P	Tyre Stiffness	160000 N/m
K_V	Piezoelectric Valve Stiffness	1140000 N/m
C_P	Tyre Viscous Damping	40 Ns/m
C_V	Piezoelectric Valve Viscous Damping	47.7 Ns/m
C_B	Variable Viscous Damping Coefficient	450 – 2000 Ns/m

The controllability matrix rank has the same order of the system dynamic matrix A . Then the system is controllable and the Riccati equation solution exists and is unique. To solve the optimization problem associated with the optimum deterministic regulator it is necessary to choose the Q and R matrices in order to determine the feedback gain matrix. Since the optimal control law has just one action force, the R matrix has one dimension. Its value is set to 10^{-2} , which produces damping forces up to the maximum allowed force at the bellows. If R is set to higher values, larger damping forces can be generated. For these cases it is important to design the bellows structure to support the mechanical stresses. The adopted design requires that the car body velocity must be reduced by the control action. This condition implies that the Q matrix element that weights this state variable must be larger than the others. The Q and R matrices presented by Equation (7) are used in all simulations.

$$Q = \begin{bmatrix} 0 & 0 & 0 & 0 \\ 0 & 0 & 0 & 0 \\ 0 & 0 & 10^6 & 0 \\ 0 & 0 & 0 & 0 \end{bmatrix} \quad \text{and} \quad R = 10^{-2} \quad (7)$$

The Riccati equation is solved and it results the feedback gain matrix: $K = [-16.75 \quad -9780.55 \quad 9583.72 \quad 91.61]$.

The local PID controller requirements were chosen to produce the valve time response less than 2 milliseconds. Additionally, the controlled system damping factor was set equal to 0.707. Using these assumptions, the PID parameters resulted: $K_P = 3.81 \cdot 10^2$, $K_I = 2.18 \cdot 10^9$ and $K_D = 13.13 \cdot 10^3$.

The simulations are done with a sampling time $\Delta t = 6.57 \times 10^{-5}$ seconds, which is a suitable rate since the maximum frequency of the system is 380 Hz, corresponding to the valve natural frequency. The vehicle speed is 80 Km/h and a hanning function is used to generate the track profile shown by Figure 6. The numerical simulations are present by figures from 7 to 12 where the results of two active systems are compared with the passive case. Figures 7 and 8 show the body car and the wheel displacements; Figures 9 and 10 show the body car and wheel velocities and Figures 11 and 12 show the passive and active damping force, the hydrodynamic valve core force and the valve displacement. Those figures will be analyzed afterward.

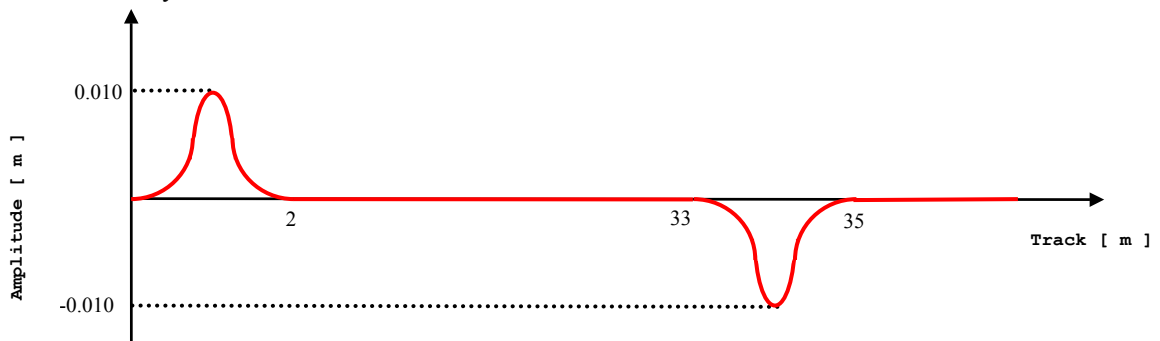


Figure 6. Rolling track profile.

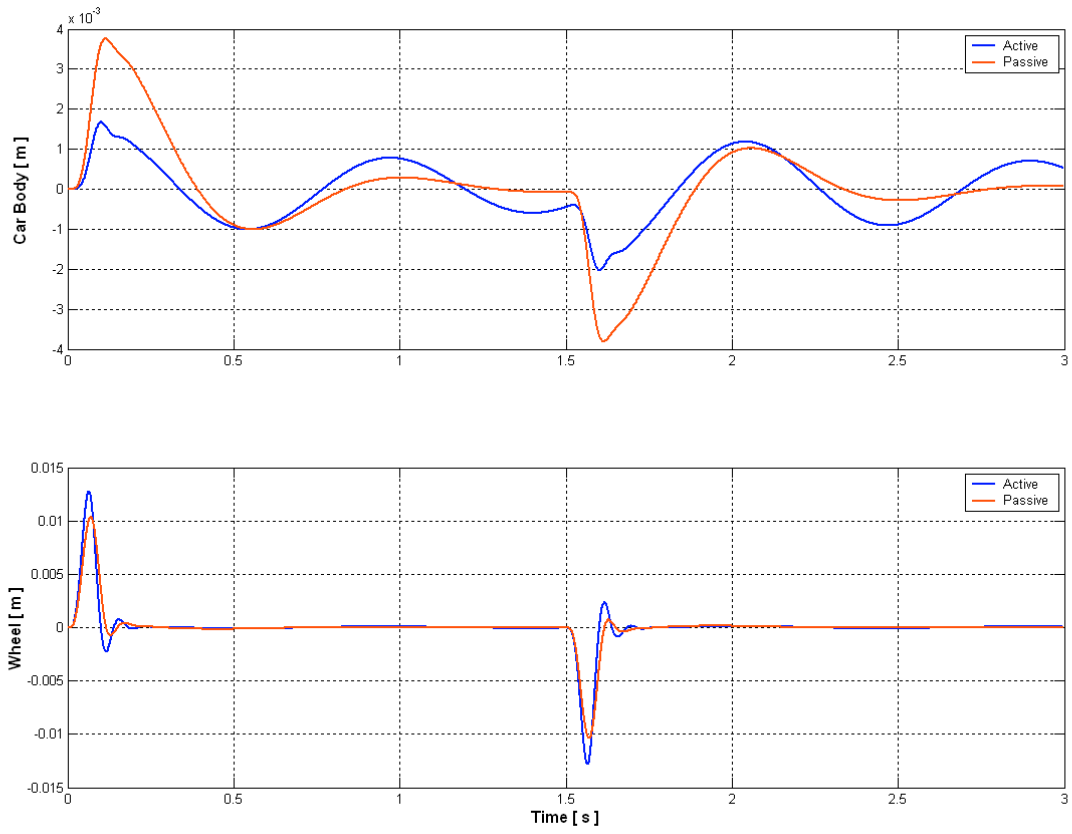


Figure 7. Displacements of the car body and wheel, with the performance index equal to 10^{-2} .

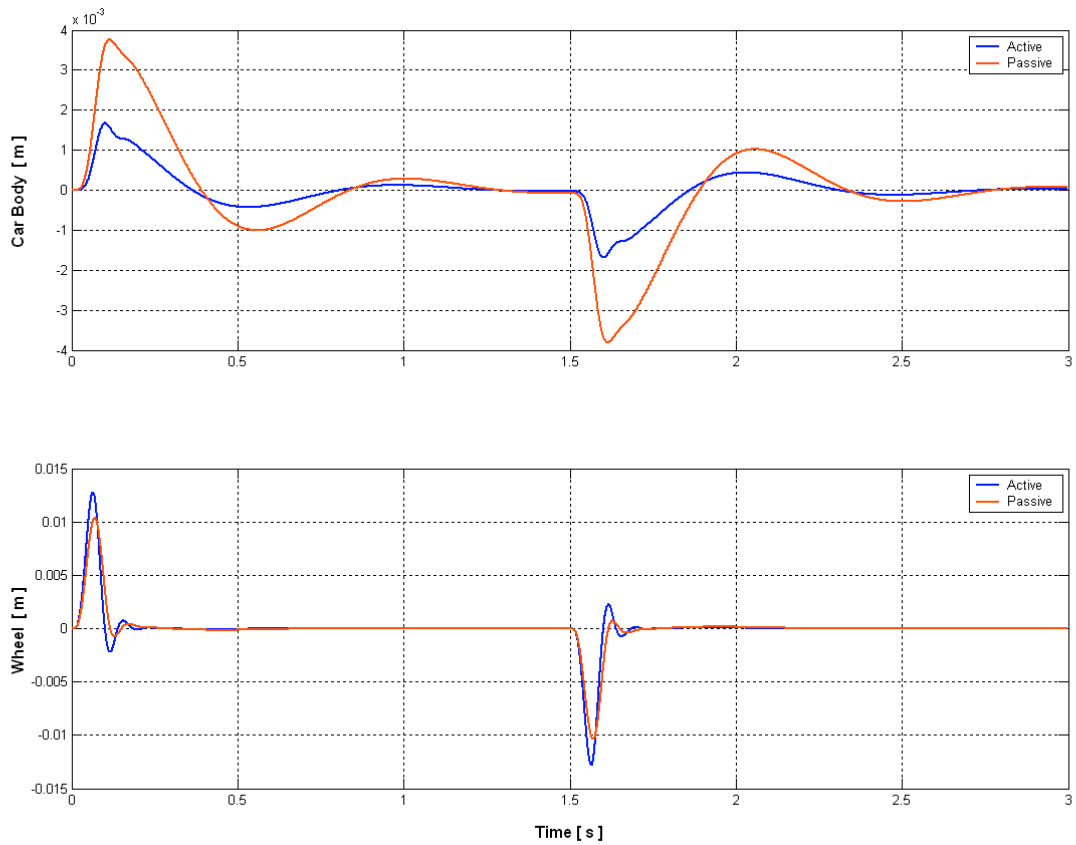


Figure 8. Displacements of the car body and wheel, with the performance index equal to 10^{-4} .

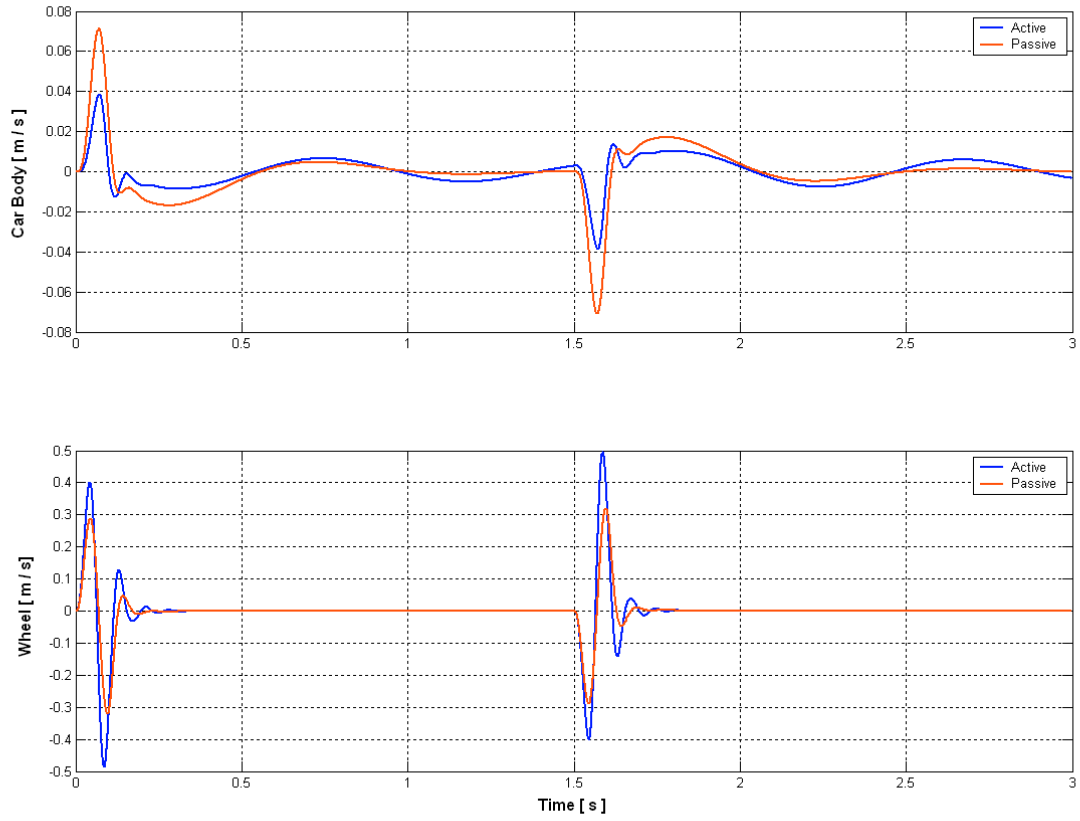


Figure 9. Velocities of the car body and wheel, with the performance index equal to 10^{-2} .

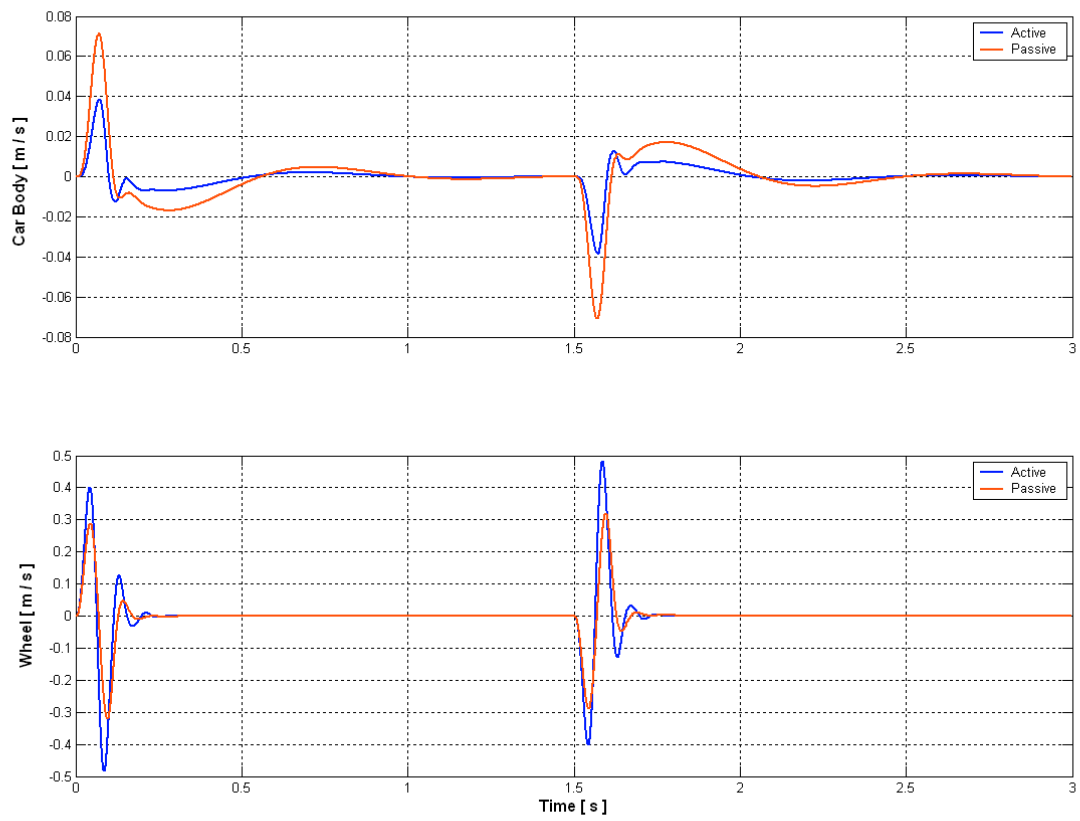


Figure 10. Velocities of the car body and wheel, with the performance index equal to 10^{-4} .

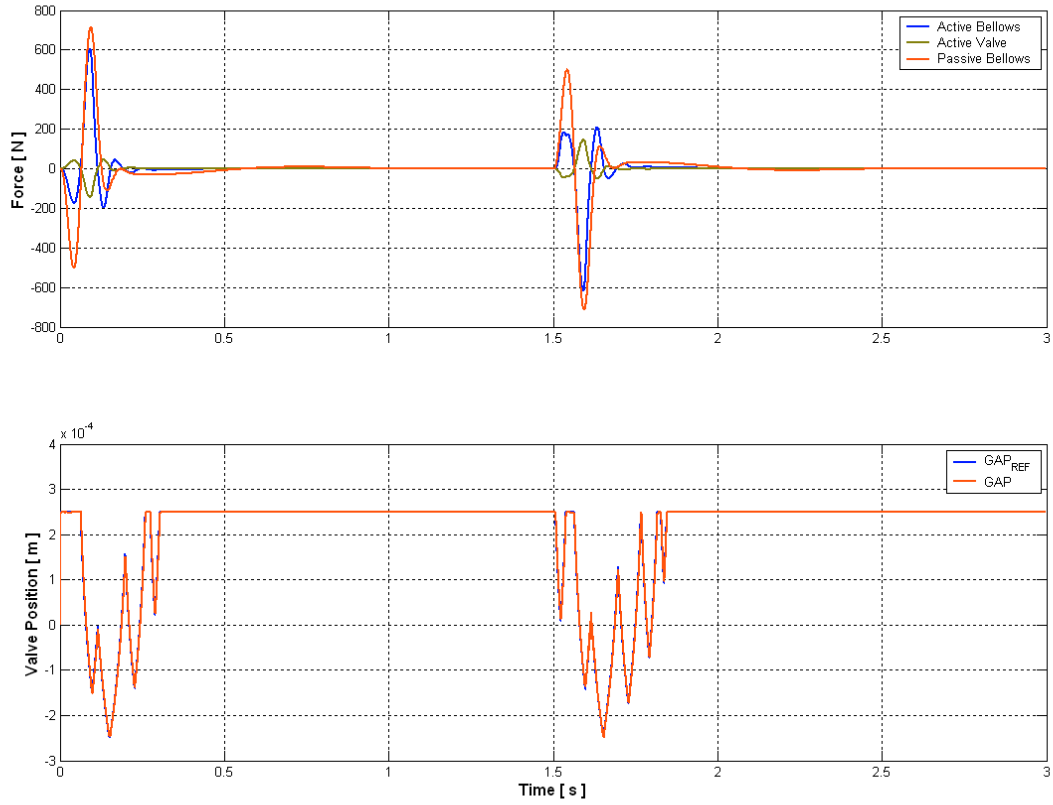


Figure 11. Active and passive forces and position of the valve core, with the performance index equal to 10^{-2} .

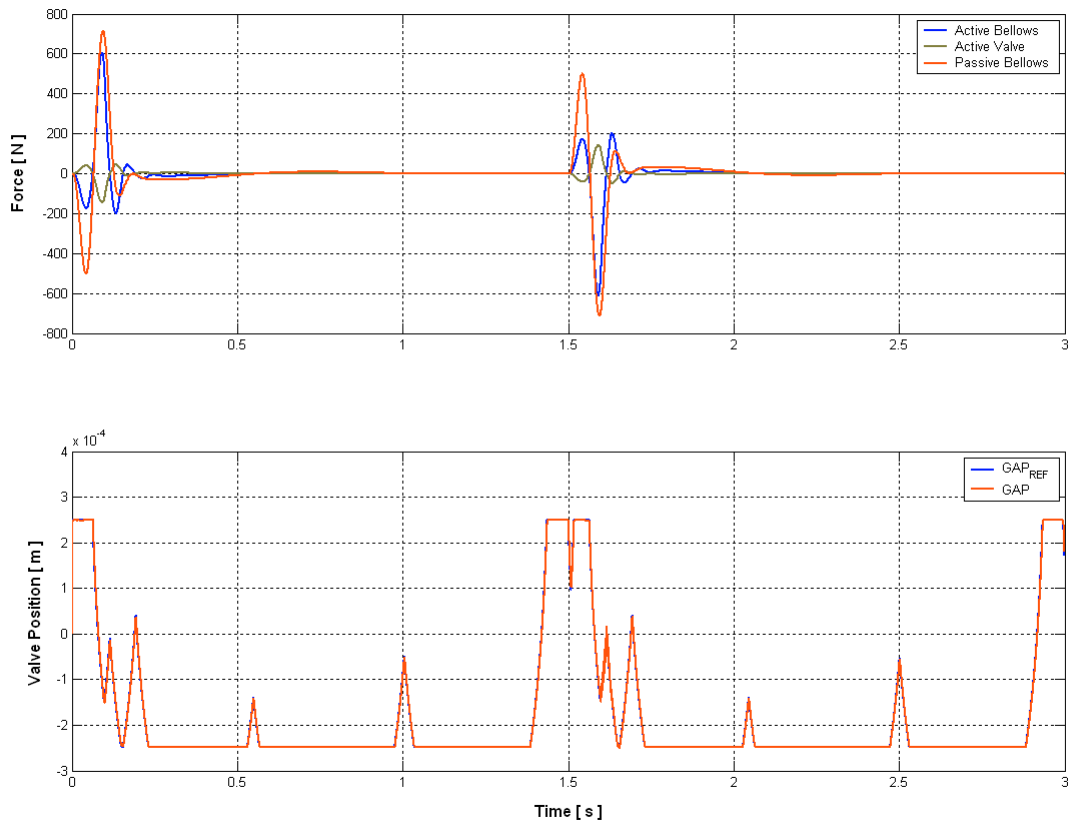


Figure 12. Active and passive forces and position of the valve core, with the performance index equal to 10^{-4} .

The RMS value of the body car displacement are calculated for each simulation and presented on Table 2. For the smaller value of the performance index the car body displacement RMS value achieve the larger reduction, compared to the passive system.

Table 2. RMS Values of Car body displacement.

SIMULATION CASE	PERFORMANCE INDEX	RMS [m]	Reduction factor [%]
Passive System	-	0.00123	-
Active System 1	0.0100	0.00077	38
Active System 2	0.0001	0.00048	61

By analyzing Figure 11 it can be seen that the control valve of the System 1 is active during a time period of approximately 0.25 seconds, on both obstacles. After the obstacles, the valve remains at its open position and the car body displacement and velocity are larger than that of the passive system, as can be seen at Figures 7 and 9. This happens because when the performance index is reached (see Figure 9), the active suspension operates with the valve at its maximum opening position, providing the minimum damping coefficient, which is smaller than the coefficient of the passive system. However, during the obstacles the active System 1 impose larger damping force providing a global reduction of 38 % on the RMS value, compared to the passive system.

The best result was obtained with system 2. In this case the valve is active during a time period of approximately 1.2 seconds, which is almost five times greater than that of System 1. During all simulation period the car body displacement and velocity are always lower than the passive case, as can be seen at Figures 8 and 10. A global reduction of 61 % on the RMS was obtained.

The control strategy did not impose any restriction on the wheel displacement. This is the reason why the wheel presents larger displacements and velocities when compared to the passive case.

The behavior of the forces acting on the bellows, which is the effective damping force, and the force at the valve core, which is directly related to the control action, can be seen at Figures 11 and 12. In all simulations the maximum values of these forces are lower than the design limits associated with the bellows strength and the force capacity of the piezoelectric actuator.

The valve displacement, presented by Figures 11 and 12 do not show clearly the PID action. The differences between the GAP_{REF} defined by the optimum controller, and the actual GAP adjusted by the PID controller, can be seen at Figure 13.

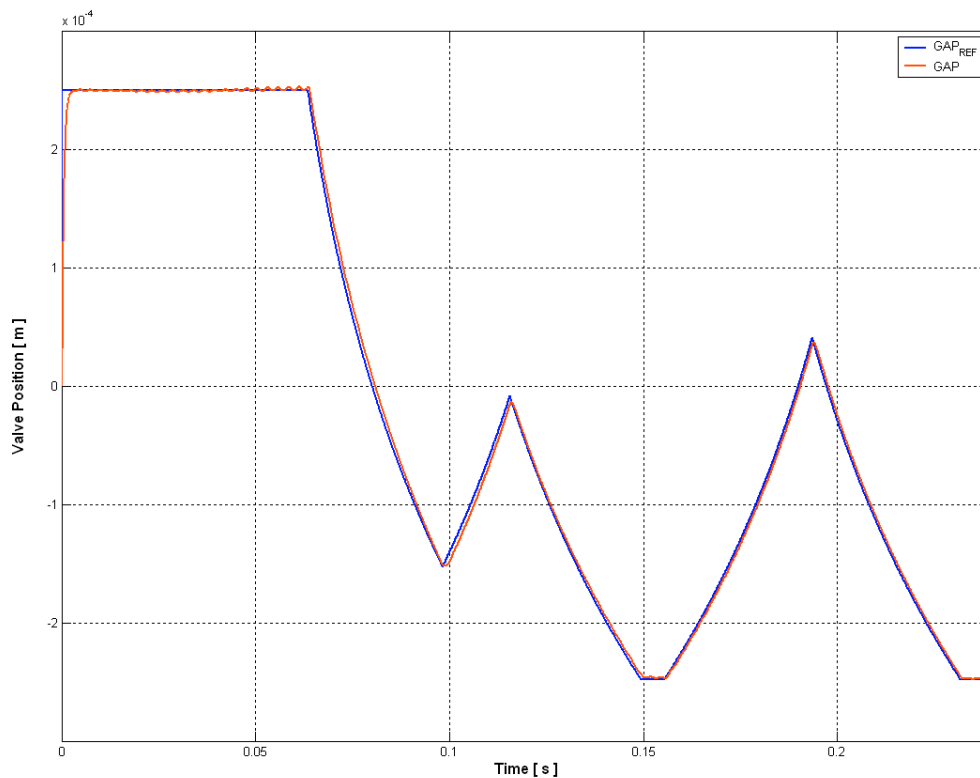


Figure 13. Detail of the PID performance for System 2.

4. Conclusion

The control strategy was defined just to reduce the car body vibrations, as imposed by the weighting Q matrix definition, which corresponds to a condition of ride comfort. Additional requirements, as for example, the force at the tyre-road contact and the wheel velocity will be included on the control design to improve the global state of the system, for case where the vehicle stability is the main goal.

The neural fuzzy and the inverse analytical models, obtained from the finite element model presented in part A of this paper, have very good computational efficiency. Despite the complexity of the hydrodynamic behavior of the damping device, the adopted reduced models can provide good estimates of the nonlinear forces and the associated valve positions, with very low computational effort.

The use of the PID local controller dedicated to the valve core positioning is a interesting solution to compose the global system controller. The optimum PID design requires higher sampling rates than that needed to capture the vehicle dynamics.

The passive system uses a fixed damping coefficient, which is the maximum coefficient generated by the damper device. This fact explains why the System 1 presented lower attenuation after the obstacles. The performance index is used to monitor the absolute value of the suspension relative velocity. The controller is deactivated when the V_x is less or equal to the specified index. The suitable choice of this index is very important to produce good dynamic response of the vehicle, as shown by the simulation of System2.

In a further work the physical limits of the actuator force values and related valve displacements can be practically realizable using an actual piezoelectric device. The proposed hierarchical control strategies will be tested on a experimental prototype that is under construction.

5. Acknowledgement

The authors thank to the financial support obtained from CAPES, CNPq and FAPEMIG Brazilian research agencies.

6. References

- Athans, M., 1971, "The Role and Use of Stochastic Linear-Quadratic-Gaussian Problem in Control System Design", Automatic Control Vol. AC-16, No 6, Dezembro.
- Cardoso, P. M. and Ribeiro, J. F., 2003, "Auto-Tuning of PID Controllers Based on the Relay Feedback Test: A New Approach – Part II", XVII COBEM, São Paulo–Brazil, In Press.
- Franklin, G.F.; Powell, J.D. and Workman M., 1997, "Digital Control of Dynamic System". Third Edition - Addison Wesley Longman, ISBN 0-201-82054-4.
- Giliomee, C.L. and Els, P.S., 1998, "Semi-active hydropneumatic spring and damper system". Journal of Terramechanics 35, pp 109-117.
- Hagopian, J. Der, Gaudiller, L. and Maillard, 1999, "Hierarchical control of hydraulic active suspensions of a fast all-terrain military vehicle". Journal of Sound and Vibration 222(5),723-752. Article No. 1998.2082, available on line at <http://www.ideallibraty.com>
- Kitching, K.J., Cole, K.J., Cebon,D., 1998, "Performance of a semi-active damper for heavy vehicles", submitted to ASME Journal of Dynamic System Measurement and Control, June.
- Teixeira, R.L. , Lépure, F. P. and Ribeiro, J. F., 2003, "Active Damper System Desing – Part A" , XVII COBEM, São Paulo–Brazil, In Press.
- Wu, Y. and Xu,B. , 1999, "Study on the Damping Fuzzy Control of Semi-active Suspension". Proceeding in IEEE 0-7803-5296-3/99, pp. 66-69.
- Yoshimura, T. , 1998, "A semi-active suspension of passenger cars using fuzzy reasoning and the field testing". International Journal of Vehicle Design, Vol.29, No. 02, pp. 150-166.

7. Copyright Notice

The author is the only responsible for the printed material included in his paper.